Vol. 608: 247–262, 2019
https://doi.org/10.3354/meps12796

MARINE ECOLOGY PROGRESS SERIES
Mar Ecol Prog Ser

Published January 3

Reconstructing sea turtle ontogenetic habitat shifts through trace element analysis of bone tissue

Matthew D. Ramirez[1,*], Jessica A. Miller[2], Eric Parks[3], Larisa Avens[4], Lisa R. Goshe[4], Jeffrey A. Seminoff[5], Melissa L. Snover[6], Selina S. Heppell[1]

[1]Oregon State University, Department of Fisheries and Wildlife, Corvallis, Oregon 97331, USA
[2]Oregon State University, Department of Fisheries and Wildlife, Coastal Oregon Marine Experiment Station, Hatfield Marine Science Center, Newport, Oregon 97365, USA
[3]AmeriCorps VISTA, Chatham Emergency Management Agency, Savannah, Georgia 31401, USA
[4]NOAA National Marine Fisheries Service, Southeast Fisheries Science Center, Beaufort Laboratory, Beaufort, North Carolina 28516, USA
[5]NOAA National Marine Fisheries Service, Southwest Fisheries Science Center, La Jolla, California 92037, USA
[6]Population Ecology Services, Pago Pago, American Samoa 96799, USA

ABSTRACT: Trace element analysis has emerged as a powerful tool to elucidate past movement and habitat use in aquatic animals, but has been underutilized in studies of non-fish species. When applied to sequentially deposited tissues (e.g. fish otoliths, sea turtle humerus bone), the technique can be used to infer aspects of an individual's ecology through time. The goal of this study was to evaluate whether trace elements could be used to reconstruct transitions between oceanic and neritic life stages in 2 species of sea turtle. We sampled the annual humerus bone growth layers of loggerhead *Caretta caretta* and Kemp's ridley *Lepidochelys kempii* sea turtles for concentrations of 7 elements (Mg, Ca, Mn, Cu, Zn, Sr, Ba) using laser ablation-inductively coupled plasma-mass spectrometry. Previous studies have demonstrated that stable nitrogen isotope ($\delta^{15}N$) values can be used to reconstruct ontogenetic shifts between oceanic (offshore) and neritic (nearshore) habitats in these species; therefore, bone $\delta^{15}N$ data were also collected for comparison. Bone strontium to calcium (Sr:Ca) and barium to calcium (Ba:Ca) ratios were significantly higher in oceanic versus neritic life stages for both species. Changes in bone elemental ratios within individuals coincided with known changes in resource use, as indicated by $\delta^{15}N$ values, and fell within the range of body sizes and ages typical for oceanic-to-neritic ontogenetic shifts in each species. We conclude that bone Sr:Ca and Ba:Ca ratios may identify oceanic versus neritic resource use in sea turtles, but that additional studies are needed to identify the specific mechanisms underpinning these differences.

KEY WORDS: Barium · Strontium · Stable nitrogen isotopes · Habitat use · Sea turtle · Migration · Bone chemistry

1. INTRODUCTION

Long-distance migrations are a common life history feature in higher-order marine taxa (Block et al. 2011, Dodge et al. 2014), but they pose a unique challenge for scientists interested in studying even the most basic aspects of a species' ecology (e.g. sea turtle 'lost' years; Carr 1952, Reich et al. 2007). In recent decades, biologging technologies and biogeochemical approaches have emerged as powerful tools for tracking animal movements over various spatiotemporal scales (Rubenstein & Hobson 2004, Wilmers et al. 2015). While biologging can provide highly detailed movement and environmental data for individ-

*Corresponding author: matthew.ramirez@oregonstate.edu

uals, it requires a considerable investment of time and money per animal for tag deployment, and in some cases reacquisition, that can restrict sampling scope and inference. In contrast, biogeochemical approaches, which rely on habitat- or diet-specific chemical differences being reflected in animal tissues, can be employed at a reduced cost and generally do not require recapture of individuals. Once validated, biogeochemical methods can provide a rapid assessment of past habitat use, diet, or physiology over days to years depending on the tissue that is sampled (Peterson & Fry 1987).

Many biogeochemical techniques have been underutilized in marine systems for the study of animal movement and habitat use (Rubenstein & Hobson 2004, Sturrock et al. 2012). For example, while bulk stable carbon ($\delta^{13}C$) and nitrogen ($\delta^{15}N$) isotope analyses are now commonly applied across marine taxa (Hobson 2007, Michener & Kaufman 2007), investigations using trace element analysis have generally been restricted to fishes (Elsdon et al. 2008, McMillan et al. 2017). Indeed, fish otolith chemical records are routinely used to identify natal origin (Thorrold et al. 2001, Brennan et al. 2015), discriminate populations (Edmonds et al. 1991, Campana et al. 1994), and reconstruct migratory pathways (Hamer et al. 2006, Baumann et al. 2015). In contrast, trace element analysis has only been applied in a handful of studies on marine mammals and sea turtles, primarily to discriminate populations (Outridge & Stewart 1999, Kunito et al. 2002, Born et al. 2003, López-Castro et al. 2013, 2014, Botta et al. 2015, Romero et al. 2017), but also to study trophic ecology (Fontaine et al. 2007, Peek & Clementz 2012). Many of these species have tissues analogous to fish otoliths and elasmobranch vertebrae—tooth dentin in marine mammals and bone tissue in sea turtles—and, in many cases, are known to make distinct changes in habitat use and diet throughout their ontogeny. Therefore, there is the potential for greater application of trace element analysis to life history reconstruction for these taxa.

Most sea turtle species migrate between oceanic and neritic habitats during their lifetime (Bolten 2003), although the amount of time spent in different habitats varies by species, population, and life stage. These ontogenetic shifts are particularly well characterized in western North Atlantic loggerhead *Caretta caretta* and Kemp's ridley *Lepidochelys kempii* sea turtles. Both species occupy oceanic habitats as small juveniles, then recruit to and maintain long-term residency in neritic habitats along continental margins as medium-to-large juveniles and adults (Bolten 2003). This habitat shift is accompanied by a diet shift from epipelagic to primarily benthic prey (Jones & Seminoff 2013). Despite this shared life history strategy, many other aspects of their ecology differ, such as geographic location of each life stage, stage duration, size and age at maturation, and variation in timing and duration of the oceanic-to-neritic habitat shift (Table 1). For example, Kemp's ridley turtles complete this habitat shift over a narrow age range (1–3 yr; Zug et al. 1997, Turtle Expert Working Group 2000), but loggerhead turtles initiate this habitat shift over a wide range of sizes (~40–70 cm straightline carapace length, SCL) and ages (7–19 yr; Avens et al. 2013, Ramirez et al. 2015). Some loggerhead turtles also oscillate between oceanic and neritic resources for multiple years before recruiting to neritic habitats (Witzell 2002, McClellan & Read 2007, Mansfield et al. 2009, Ramirez et al. 2015).

Stable nitrogen isotope analyses can be used to reconstruct oceanic-to-neritic habitat shifts in both loggerhead and Kemp's ridley sea turtles (Snover 2002, Snover et al. 2010, Avens et al. 2013, Goodman Hall et al. 2015, Ramirez et al. 2015). Contrasting sources of nitrogen for primary production between occupied habitats (oceanic: N_2 fixation; neritic: riverine nitrate input) yield lower $\delta^{15}N$ values in the tissues of oceanic-stage turtles relative to neritic-stage turtles (Montoya et al. 2002, McKinney et al. 2010, Dorado et al. 2012). While $\delta^{15}N$ analyses have greatly expanded our ability to characterize broad-scale patterns of resource use in sea turtles, the method provides lower geographic and temporal resolution than alternative methods (e.g. satellite telemetry) (Pearson et al. 2017), prompting interest in identifying additional biogeochemical methods for geographic location assignment. For example, López-Castro et al. (2013, 2014) showed that a suite of elements can be used to identify oceanic foraging grounds of green sea turtles *Chelonia mydas* at greater spatial resolution (i.e. regions within ocean basins) than $\delta^{13}C$ and $\delta^{15}N$ values alone.

Elements that substitute for Ca^{2+} in the hard parts of animals (e.g. strontium [Sr] and barium [Ba]) typically reflect either water chemistry (otolith aragonite; Walther & Thorrold 2006) or diet (bone hydroxyapatite; Schroeder et al. 1972). Ba and Sr, in particular, have garnered widespread use as tracers of diadromous fish migrations because their abundances tend to relate to salinity (Campana 1999, Campana & Thorrold 2001, Elsdon et al. 2008). Ba is generally more abundant in freshwater, whereas Sr is generally more abundant in seawater (Coffey et al. 1997, Zimmerman 2005), although some freshwater

Table 1. Summary of pertinent life history characteristics for western North Atlantic loggerhead *Caretta caretta* (Cc) and Kemp's ridley *Lepidochelys kempii* (Lk) sea turtles. SCL: straightline carapace length

Life history characteristic	Species	Sea turtle life stage		
		Oceanic juvenile	Neritic juvenile	Adult
Habitat use[a]	Cc	Epipelagic; central Atlantic Ocean, Sargasso Sea	Benthic; US Atlantic continental shelf	Benthic; US Atlantic continental shelf
	Lk	Epipelagic; central Gulf of Mexico	Benthic; US Atlantic and Gulf of Mexico continental shelf	Benthic; US Atlantic and Gulf of Mexico continental shelf
Life stage duration (yr)	Cc	8–12[b,c]	15–25[d]	4–46[d]
	Lk	1–3[e,f]	8–12[g]	1–10[g]
Approximate size range (cm SCL)	Cc	5–50	50–90	>90
	Lk	5–25	25–60	>60
Approximate age range (yr)	Cc	0–10	10–35	>35
	Lk	0–2	2–10	>10
Nesting location	Cc	—	—	US Atlantic Coast; Florida to North Carolina
	Lk	—	—	Western Gulf of Mexico; Texas and Mexico

[a]Bolten (2003), [b]Avens et al. (2013), [c]Bjorndal et al. (2000), [d]Avens et al. (2015), [e]Zug et al. (1997), [f]Turtle Expert Working Group (2000), [g]Avens et al. (2017)

sources can have Sr concentrations similar to seawater (Kraus & Secor 2004). Within fully marine systems, and particularly the open ocean, seawater Sr and Mg concentrations are relatively homogeneous and can be poor geographic tracers (de Villiers 1999, Foster et al. 2010, Peek & Clementz 2012). Ba concentrations, in contrast, exhibit greater spatial heterogeneity (Peek & Clementz 2012, Sturrock et al. 2012). Multiple studies have observed increases in otolith Ba:Ca ratios in fish that migrate from coastal habitats to bays/estuaries (Hamer et al. 2006, Fowler et al. 2016) or open ocean to coastal habitats (Hamilton & Warner 2009, Baumann et al. 2015).

Both environmental and physiological factors can influence elemental incorporation in complex and sometimes multiplicative ways (Kalish 1991, Elsdon & Gillanders 2003). Temperature and growth can independently and jointly have strong effects (positive, negative, neutral) on otolith Sr and Ba incorporation (e.g. Bath et al. 2000, Elsdon & Gillanders 2002, DiMaria et al. 2010). Similarly, ontogenetic and taxonomic effects can explain significant variation in elemental ratios within and among fish species (Walther et al. 2010, Chang & Geffen 2013). Direct assessments of these and other factors are generally lacking for elasmobranch vertebrae, marine mammal teeth, and sea turtle bones (but see Smith et al. 2013). Furthermore, discrimination against Sr and Ba relative to Ca during metabolic processing result in decreasing Sr:Ca and Ba:Ca ratios with increasing trophic level (Burton et al. 1999, Peek & Clementz 2012). Therefore, variation in elemental ratios within species that primarily obtain trace elements through their diets, such as marine mammals and sea turtles, may reflect differences in diet, habitat, or both.

In this study, we analyzed the humerus bones of loggerhead and Kemp's ridley sea turtles via laser ablation-inductively coupled plasma-mass spectrometry (LA-ICP-MS) to evaluate whether trace element ratios can be used to reconstruct transitions between oceanic and neritic life stages in sea turtles. The primary objectives of this study were to (1) quantify within-species variation in elemental ratios relative to turtle size and age and (2) determine if changes in elemental ratios coincide with changes in $\delta^{15}N$ values reflecting oceanic-to-neritic movements. These species make ideal candidates for this study because they undertake distinct, well-studied transitions between oceanic and neritic habitats as juveniles (Bolten 2003; Table 1). They also contain annual chemical records in their bone tissue for multiple years prior to death, although bone resorption usually prevents the reconstruction of complete life histories for most individuals (Zug et al. 1986). In addition, previous studies have demonstrated that $\delta^{15}N$ values can be used to reconstruct the oceanic-to-

neritic habitat shift in these species (Snover 2002, Snover et al. 2010, Avens et al. 2013, Goodman Hall et al. 2015, Ramirez et al. 2015), providing a metric for comparison between the 2 methods. LA-ICP-MS has the potential for quantifying within-year chemical variation in sampled tissues, an advantage over micromilling techniques used for stable isotope analysis, which require integration over whole growth layers (but see Moran et al. 2011). If trace elements can be used to reconstruct habitat use in sea turtles, and if factors influential to elemental incorporation in tissues can be identified, this technique may provide a means of assigning past geographic location for animals at multiple spatial scales.

2. MATERIALS AND METHODS

2.1. Sample collection and skeletochronology

Humerus bones were collected from dead stranded turtles (1997–2011) through the US National Sea Turtle Stranding and Salvage Network (https://www.sefsc.noaa.gov/species/turtles/strandings.htm). Loggerhead bones (juvenile: n = 35, adult: n = 18) were collected on beaches from North Carolina to New Jersey and Kemp's ridley bones (n = 44, all juvenile) were collected on beaches from Texas to Virginia. Stranding location, date, and SCL (measured as the straightline distance from the nuchal notch to the posterior tip of the carapace) were collected at time of stranding. When only curved carapace length was measured, SCL was estimated following Snover et al. (2010) for loggerheads (n = 1) and Snover et al. (2007b) for Kemp's ridleys (n = 8). Maturity status was determined through visual examination of gonads during necropsy or was based on record of nesting using tagging data. Sample characteristics of stranded turtles are presented in Table 2.

All turtle bones included in this study were histologically processed in previous skeletochronology studies (Snover et al. 2007b, 2010, Avens et al. 2013, 2017, Ramirez et al. 2015) using standard methods (Avens & Snover 2013; see Text S1 in the Supplement at www.int-res.com/articles/suppl/m608p247_supp.pdf). Briefly, 2 sequential cross-sections were collected from each bone: 1 for skeletochronology and 1 for chemical analysis. Following histological processing, digital images of each hematoxylin-stained bone thin-section were examined by 2 independent readers to determine the number and placement of lines of arrested growth (LAGs), which delimit the outer edges of each skeletal growth mark. LAGs are deposited annually in these species (e.g. Avens et al. 2013, 2017).

An allometric relationship exists between humerus section diameter (HSD) and SCL for both species (Snover et al. 2007a, Avens et al. 2017). These relationships were combined with the body proportional hypothesis (Francis 1990) to estimate SCL for every measurable LAG, adjusted for turtle-specific SCL and HSD at death. A mean SCL estimate was generated for each growth layer and used for all analyses. In addition, we quantified age at stranding using either a direct count of LAGs if the first-year annulus was still visible (true age) or direct counts in combination with a correction factor to estimate the number of LAGs lost to resorption (estimated age; see the Supplement). Age at stranding was then used to back-assign true or estimated age to LAGs. True age was not known for loggerhead turtles included in this study due to their extended oceanic life stage and resorption of the first-

Table 2. Sample characteristics for stranded sea turtles and sampled bone growth layers. Maturity status was determined through necropsy or observation of nesting. SCL: straightline carapace length, Me: metal

Species	Turtle sample size	SCL at stranding (cm) Mean ± SD (range)	Estimated age at stranding (yr) Mean ± SD (range)	Unique bone growth layers sampled	
				$\delta^{15}N$	Me:Ca
Loggerhead, juvenile	35	66.9 ± 9.6 (51.2–86.8)	16.85 ± 3.95 (11.00–26.75)	228	248
Loggerhead, adult	18	95.3 ± 5.1 (84.9–103.0)	53.57 ± 12.54 (36.25–77.00)	0[a]	18[b]
Kemp's ridley, juvenile	44	41.6 ± 5.3 (30.6–50.5)	4.69 ± 1.04 (3.75–8.25)	124	97

[a]Growth layers too narrow to sample individually for $\delta^{15}N$ values
[b]Data averaged across each ablation transect

year growth mark, thus ontogenetic comparisons for loggerhead turtles were made based on size. In contrast, true age was known for most Kemp's ridley turtles sampled, so age was used for ontogenetic comparisons. Given that LAG deposition occurs in late winter/early spring and peak hatching occurs during the summer (Snover & Hohn 2004), the first-year growth mark denotes an age of ~0.75 yr, the next LAG an age of 1.75 yr, and so on (see the Supplement).

2.2. Stable nitrogen isotope analysis

Differences in nitrogen cycling between oceanic and neritic habitats occupied by loggerhead and Kemp's ridley sea turtles yield divergent baseline $\delta^{15}N$ values that are transferred to consumers (Dorado et al. 2012, McMahon et al. 2013). The principal sources of nitrogen for primary production in occupied oceanic and neritic habitats are N_2 fixation and riverine inputs, respectively (Montoya et al. 2002, McKinney et al. 2010, Dorado et al. 2012). As N_2 fixation reduces $\delta^{15}N$ values, tissues collected from consumers in western North Atlantic and central Gulf of Mexico oceanic habitats tend to have lower $\delta^{15}N$ values relative to conspecifics in neritic habitats (Wells & Rooker 2009, Dorado et al. 2012). For loggerhead and Kemp's ridley sea turtles, these differences manifest as sharp increases in $\delta^{15}N$ values within tissues following the oceanic-to-neritic life stage transition (Snover 2002, Snover et al. 2010, Avens et al. 2013, Goodman Hall et al. 2015, Ramirez et al. 2015). Therefore, $\delta^{15}N$ values were used as a secondary measure of individual resource use through time against which trace element data were compared.

Only juvenile turtles were sampled for $\delta^{15}N$ values, given that adult growth layers were too narrow to sample individually. Bone dust (~1.6 mg) was collected from each annual growth increment using a micromill (ESI New Wave Research) and analyzed for $\delta^{15}N$ values by a continuous-flow isotope-ratio mass spectrometer at Oregon State University, Corvallis, OR (see Text S1 in the Supplement). Transparencies of the digital skeletochronology images were used to guide drilling of cortical bone to a depth of ≤1.0 mm. A 0.4 mm diameter carbide drill bit (Brasseler) was used to ensure sampling of individual growth layers. Each sample was considered an integration over each growth year, and bulk bone $\delta^{15}N$ values were assumed to reflect that of bone collagen (Turner Tomaszewicz et al. 2015). C:N ratios were below 3.5, characteristic of unaltered protein (Koch et al. 1994) with low lipid content (Post et al. 2007). Loggerhead isotopic data herein were previously presented by Ramirez et al. (2015) to characterize the loggerhead oceanic-to-neritic ontogenetic shift, but are used here to gain novel insight into the use of additional chemical tracers to reconstruct this life stage transition.

2.3. Trace element analysis

Following micromilling, bone cross-sections were polished (240–1200 grit sandpaper, lapping film, and AlO_2 powder), cleaned ultrasonically in Nanopure water, and mounted onto glass slides. Bone ^{24}Mg, ^{43}Ca, ^{55}Mn, ^{65}Cu, ^{66}Zn, ^{86}Sr, and ^{138}Ba were quantified using a Thermo Elemental X-Series II ICP-MS coupled with a New Wave DUV193 excimer laser at Oregon State University's WM Keck Collaboratory for Plasma Spectrometry in Corvallis, OR. The laser was set at a pulse rate of 5 Hz with a spot size of 15–20 µm and a travel rate of 10 µm s^{-1} for juvenile bones (both species) and 5 µm s^{-1} for adult bones (loggerhead). All transects were pre-ablated at a pulse rate of 2 Hz with a spot size of 85 µm to remove surface contamination. Trace element profiles were collected from the inner part of the bone (older growth layers) to the outer part of the bone (newer growth layers; Fig. 1).

Background levels of analytes were measured for 45 s prior to bone ablation and subtracted from count rates measured during ablation. Count rates for each analyte were normalized to ^{43}Ca to account for variation in instrument sensitivity and ablation rate. NIST 612 standard glass was used to convert normalized ion ratios to elemental ratios and to quantify precision (Kent & Ungerer 2006, Miller 2007, Jochum et al. 2011). Bone metal to calcium ratios (Me:Ca) are reported in mg g^{-1}. The mean percent relative standard deviations for NIST 612 glass during data collection were ^{24}Mg = 12.0%, ^{55}Mn = 7.9%, ^{65}Cu = 12.5%, ^{66}Zn = 18.3%, ^{86}Sr = 6.9%, and ^{138}Ba = 8.4%. A calcium carbonate standard of known composition prepared by the United States Geological Survey (USGS MACS-1) provided an estimate of accuracy. Measured values differed from known values by 9.6 ± 1.3% (mean ± SE) for Mn:Ca, 0.2 ± 3.0% for Cu:Ca, 45.0 ± 6.6% for Zn:Ca, 1.0 ± 0.8% for Sr:Ca, and 8.2 ± 1.5% for Ba:Ca. Mg:Ca is not homogeneous in MACS–1 and was therefore not evaluated.

Following LA-ICP-MS, ablation transects were digitally imaged. Digital post-ablation images for each bone were overlaid onto 'skeletochronology' images in Adobe Photoshop (Adobe Systems). The distance

from the start of the ablation line to each LAG was then measured and used to assign segments of each elemental profile to individual growth increments. For sampled juveniles, mean elemental ratios (Me:Ca) were calculated for each growth increment to allow for comparison with $\delta^{15}N$, size, and age data. For sampled adults, growth layers were too compressed to allow for the accurate assignment of data to individual growth increments, so data were averaged across whole transects.

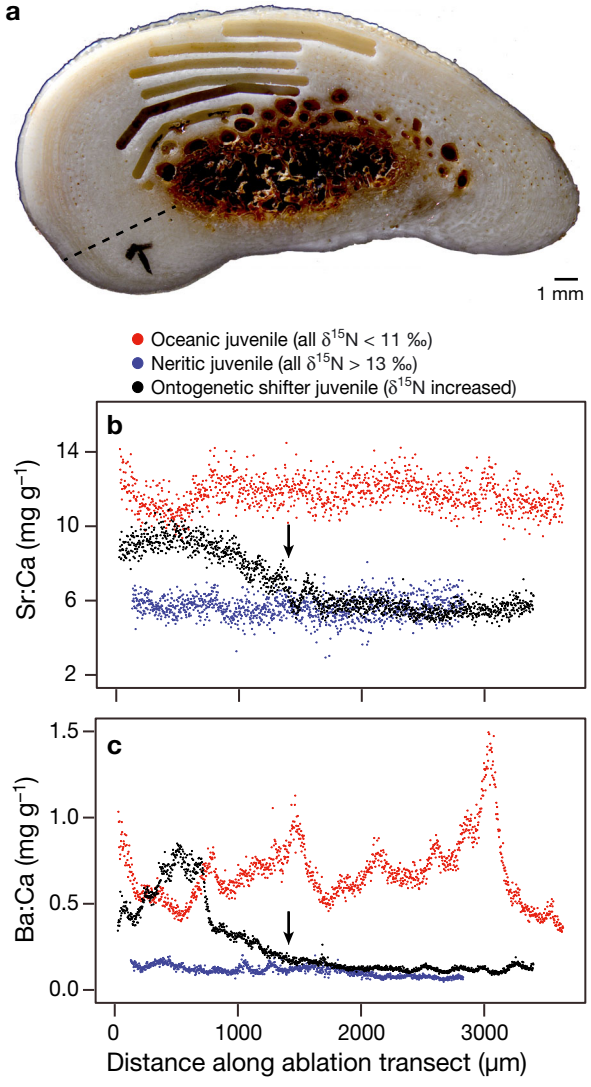

Fig. 1. (a) Loggerhead sea turtle bone cross-section sampled for $\delta^{15}N$ values (micromilled lines) and trace element ratios (dashed line above arrow). (b,c) Example elemental profiles for 3 loggerhead turtles. The small oceanic juvenile (red points) displayed consistently low bone $\delta^{15}N$ values (<11.0‰), indicative of consistent oceanic habitat use in the years prior to death, whereas the large neritic juvenile (blue points) displayed consistently high bone $\delta^{15}N$ values (>13.0‰), indicative of consistent neritic habitat use in the years prior to death. (Note that the oceanic-to-neritic shift was likely not observed in this turtle due to bone resorption of transitional growth layers.) The ontogenetic-shifter juvenile (black points) displayed a marked increase in bone $\delta^{15}N$ values consistent with the oceanic-to-neritic life stage transition. Black arrows denote the midpoint of the growth increment associated with the start of the ontogenetic shift based on change in $\delta^{15}N$ values

2.4. Statistical analyses

All statistical analyses were implemented in R version 3.4.4 (R Core Team 2018). Before statistical tests were performed, data were tested for normality and homogeneity of variances using Shapiro-Wilk and Levene's tests. In most cases, elemental ratios were $\log_{10}$-transformed to meet parametric assumptions (Table 3, and see Table S1 in the Supplement). Generalized additive mixed models (GAMMs) were used to initially characterize relationships between elemental ratios and body size (loggerhead) or age (Kemp's ridley). As described previously, we used body size for loggerhead analyses and age for Kemp's ridley analyses because true age was unknown for sampled loggerhead turtles but known for most sampled Kemp's ridley turtles (see Section 2.1). Within each species, separate models were built for each elemental ratio using the 'mgcv' package that included either size or age as a fixed effect, turtle-specific random effects, and first-order autoregressive [AR(1)]

Table 3. Statistical output for linear mixed models (LMMs) used to examine the effect of back-calculated straightline carapace length (SCL) 10 cm size class (juvenile loggerheads, n = 35) or age class (juvenile Kemp's ridleys, n = 44) on bone isotopic ($\delta^{15}N$) and elemental ratios. General model: lme($\delta^{15}N$ ~ size or age class, random = ~1|Bone_ID, correlation = corAR1(form = ~1| Bone_ID)). Results of Tukey's post hoc multiple comparisons presented in Table S2. N: number of unique bone growth layers included in the analysis, numDF (denDF): numerator (denominator) degrees of freedom. **Bold:** significant

Model	N	numDF	denDF	*F*	p
Loggerhead sea turtles					
$\delta^{15}N$ ~ size class	228	5	188	15.74	**<0.001**
Mg:Ca[a] ~ size class	248	5	208	4.00	**0.002**
Sr:Ca ~ size class	248	5	208	5.90	**<0.001**
Ba:Ca[a] ~ size class	248	5	208	6.14	**<0.001**
Kemp's ridley sea turtles					
$\delta^{15}N$ ~ age class	124	5	79	15.65	**<0.001**
Mg:Ca[a] ~ age class	97	5	60	0.92	0.478
Sr:Ca ~ age class	97	5	60	8.54	**<0.001**
Ba:Ca[a] ~ age class	97	5	60	7.56	**<0.001**

[a]Data were log10-transformed prior to analysis

covariance structure (Wood 2006). These initial models revealed changes in some trace element ratios with increasing size (loggerhead) or age (Kemp's ridley; Fig. 2, Table S1).

To allow for more precise statistical comparisons among sizes and ages, data were binned by 10 cm size class (loggerhead) or annual age class (Kemp's ridley) and compared using general linear mixed models (GLMMs) and post hoc Tukey's multiple comparisons tests. As is common practice for sea turtle studies, loggerhead growth increments and their associated data were binned into size classes (30 to 80 cm SCL) based on the mean back-calculated SCL for each growth increment (i.e. 30 cm size class includes data for growth increments with mean back-calculated SCL between 30.0 and 39.9 cm). Kemp's ridley growth increments and their associated data were binned into annual age classes based on turtle age at the beginning of the growth increment (i.e. 1.75 age class is the growth layer from age 1.75 to 2.75). As with the GAMMs, separate models were built for each elemental ratio that included turtle-specific random effects and AR(1) covariance structure. GLMMs and multiple comparison tests were implemented using the 'nlme' and 'multcomp' packages in R (Hothorn et al. 2008, Pinheiro et al. 2018).

Because elemental data collected for adult loggerheads were at lower resolution than for juveniles, 2 additional sets of linear mixed models were developed to compare elemental ratios among life stages within each species (e.g. oceanic juvenile vs. neritic juvenile vs. adult). To this end, species-specific models were generated with juvenile data binned into life stages based on $\delta^{15}N$ values for loggerhead turtles and ages for Kemp's ridley turtles. Loggerhead bone $\delta^{15}N$ values <11.0 and >13.0‰ are generally consistent with oceanic and neritic resource use, respectively (Ramirez et al. 2015). These thresholds were used to assign individual growth increments to

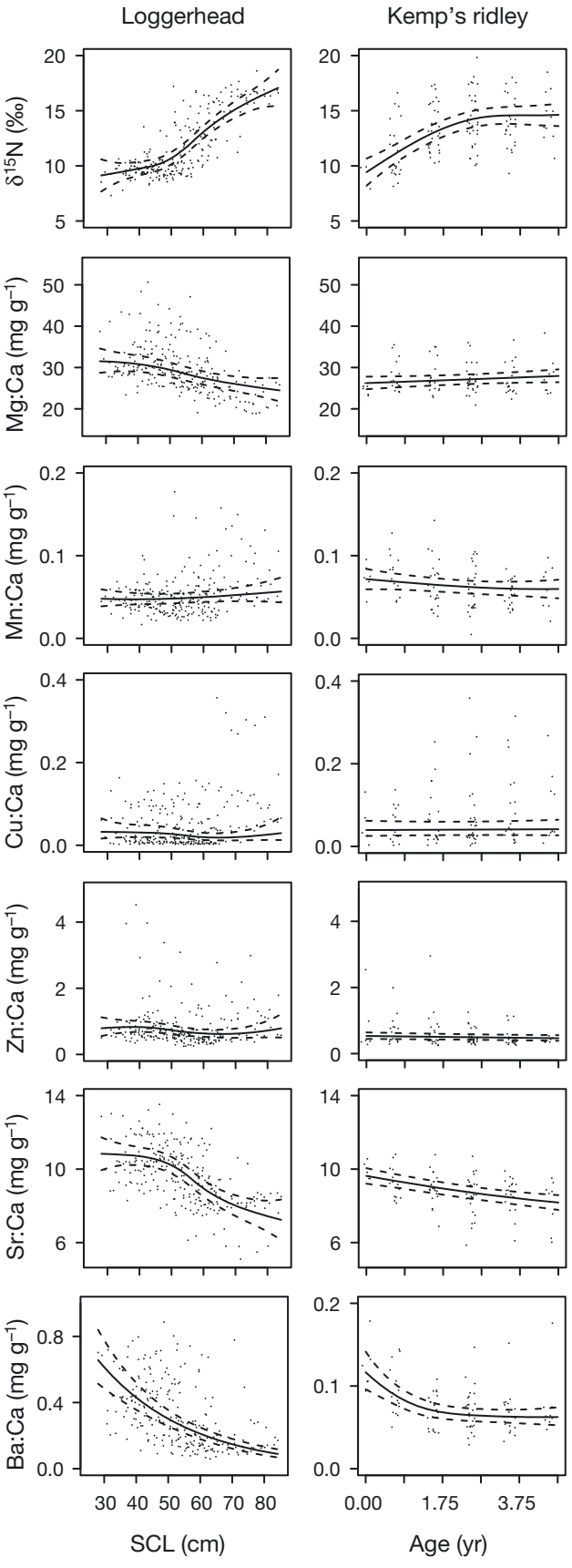

Fig. 2. Generalized additive mixed model (GAMM) estimated smoothing curves (solid lines) and 95% confidence intervals (dashed lines) for models comparing isotopic ($\delta^{15}N$ values) and elemental ratios and back-calculated straight-line carapace length (SCL; loggerhead, left column) or age (Kemp's ridley, right column). Points are data for individual growth increments. Data presented are for all sampled juvenile turtles, including oceanic, neritic, and ontogenetic shifters and are untransformed. Kemp's ridley data are jittered to allow for better visualization. Statistical output is presented in Table S1 in the Supplement. Note different *y*-axis ranges for Ba:Ca ratios

oceanic ('Cc oceanic juvenile') or neritic juvenile life stages ('Cc neritic juvenile'). Kemp's ridley turtles generally transition between oceanic and neritic habitats between the ages of 1 and 3, thus growth increments with age assignments of 0.00 were assigned to the oceanic juvenile life stage ('Lk oceanic juvenile') and growth increments with age assignments ≥2.75 were assigned to neritic juvenile life stages ('Lk neritic juvenile'). Classification based on age was chosen for Kemp's ridley sea turtles given the narrow range of ages at which they are expected to transition to neritic habitats, and because no previous classification based on $\delta^{15}N$ values has been developed.

Lastly, correlation analyses were used to characterize the relationship between $\delta^{15}N$ values and trace element ratios. Because our data were non-independent, a repeated measures correlation analysis (rmcorr) was performed using the 'rmcorr' package in R (Bakdash & Marusich 2017). The technique uses analysis of covariance (ANCOVA) to account for between-turtle variation, a distinction from other correlation analyses (e.g. Pearson, Spearman), and generates a common regression slope and best linear fits for each turtle with the same slope but different intercepts. As with the Pearson correlation coefficient (r), the rmcorr coefficient (r_{rm}) quantifies the strength of the linear relationship between 2 continuous variables and ranges from −1 to 1.

3. RESULTS

3.1. Stable nitrogen isotope data

Stable nitrogen isotope values ranged from 7.31 to 18.61‰ for juvenile loggerhead sea turtles and from 7.92 to 19.83‰ for juvenile Kemp's ridley sea turtles. No adult turtles were sampled for $\delta^{15}N$ values. Loggerhead $\delta^{15}N$ values exhibited a pronounced increase in the 50 cm SCL size class (Fig. 2), which aligns with current estimates of mean size at transition between oceanic and neritic resources in this species (~45–55 cm SCL; see Avens et al. 2013 for review). Kemp's ridley $\delta^{15}N$ values similarly increased in the 0.75 and 1.75 age classes and plateaued after the 2.75 age class, aligning with a presumed oceanic residence of 1–3 yr for this species (Zug et al. 1997, Turtle Expert Working Group 2000). These increases in $\delta^{15}N$ values with size and age conform with expected changes in turtle tissue $\delta^{15}N$ values as turtles migrate from oceanic habitats with relatively low baseline $\delta^{15}N$ values to neritic habitats with relatively high baseline $\delta^{15}N$ values within the North Atlantic Ocean and Gulf of Mexico (Dorado et al. 2012, McMahon et al. 2013, Ramirez et al. 2015).

3.2. Ontogenetic changes in elemental ratios

GAMMs characterizing the relationship between bone trace element ratios and body size (loggerhead) or age (Kemp's ridley) showed significant non-linear trends for Sr:Ca and Ba:Ca ratios in both species, and for the Mg:Ca ratios in juvenile loggerheads only (Table S1, Fig. 2). While $\delta^{15}N$ values increased with size or age, Mg:Ca, Sr:Ca, and Ba:Ca ratios generally decreased. Inflection points in these relationships tended to occur at similar sizes and ages, suggesting inverse relationships between $\delta^{15}N$ values and Mg:Ca, Sr:Ca, and Ba:Ca ratios (see below). Relationships between juvenile loggerhead body size and Cu:Ca and Zn:Ca ratios were also statistically significant (<0.05; Table S1), but further analysis revealed that these relationships were driven by outliers in the data. For this reason, and because 95% confidence intervals tended to overlap with increasing size or age (Fig. 2), Cu:Ca and Zn:Ca, along with Mn:Ca ratios, were excluded from further analysis. Full elemental profiles for Mg:Ca, Sr:Ca, and Ba:Ca ratios for all individual turtles sampled are presented in Figs. S1–S3.

Tukey's post hoc multiple comparison tests revealed significant differences in mean bone elemental ratios among sea turtle size and age classes (Fig. 3, Table S2). As with the $\delta^{15}N$ data, mean Mg:Ca, Sr:Ca, and Ba:Ca ratios began to decrease in the 50 cm SCL size class for loggerhead turtles and the 0.75 and 1.75 yr age class for Kemp's ridley turtles (Fig. 3, Table S3; Tukey's post hoc $p < 0.05$). Elemental ratios were consistently higher in the size (30 and 40 cm SCL) and age (0.00 yr) classes preceding this shift and consistently lower in the size (60 to 80 cm SCL) and age (2.75 to 4.75 yr) classes following this shift, inverse to changes in mean $\delta^{15}N$ values with size and age class (Fig. 3). The Ba:Ca ratio exhibited the greatest ontogenetic changes in both species, reducing in mean value by approximately half throughout ontogeny. With the exception of Sr:Ca in loggerhead turtles, declines in Mg:Ca and Sr:Ca ratios were less distinct for both species.

Within loggerhead turtles, Tukey's post hoc multiple comparison tests showed that bone elemental ratios did not differ between neritic juvenile and adult life stages (Fig. 4; $p_{Mg:Ca} = 0.28$, $p_{Sr:Ca} = 0.98$, $p_{Ba:Ca} = 0.34$). This was expected, given that they co-

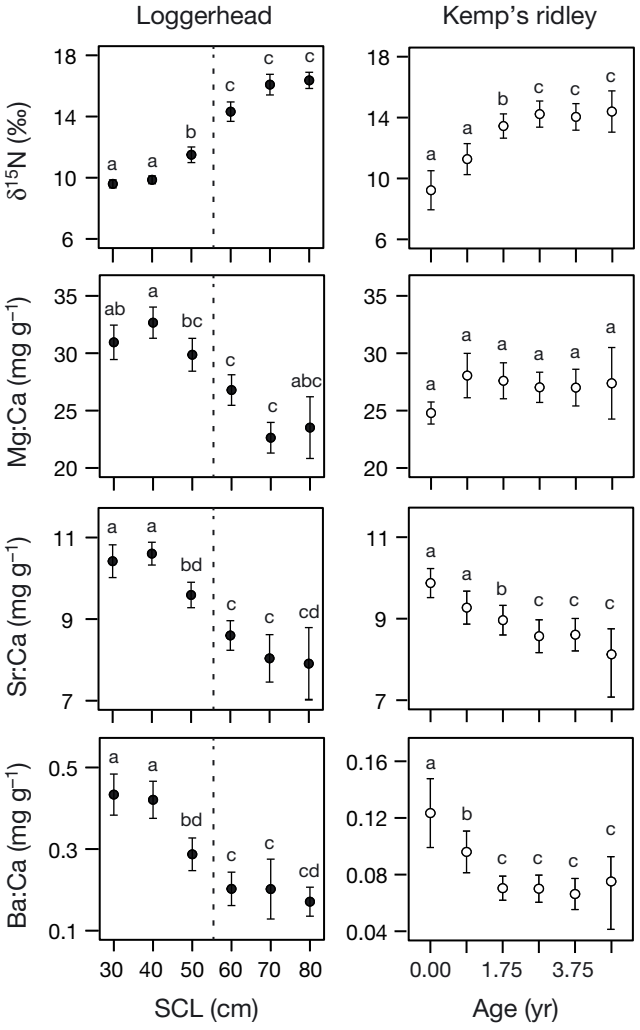

Fig. 3. Mean size- or age class-specific $\delta^{15}N$ values and Mg:Ca, Sr:Ca, and Ba:Ca ratios for loggerhead (left column, filled circles) and Kemp's ridley (right column, open circles) sea turtles. Data presented are for all sampled juvenile turtles, including oceanic, neritic, and ontogenetic shifters and are untransformed. Error bars are 95% confidence intervals, and different letters represent significant differences as determined by Tukey's post hoc multiple comparison tests (see Table S2 in the Supplement). Dashed line is mean size at oceanic-to-neritic transition for loggerheads (Avens et al. 2013, Ramirez et al. 2015). Sample sizes are presented in Table S3. Note different *y*-axis ranges for Ba:Ca ratios

occur and forage on similar resources in neritic habitats. Bone elemental ratios were significantly different between oceanic and neritic life stages within each species (Fig. 4; Tukey's post hoc $p < 0.05$). Interestingly, the maximum Ba:Ca ratio observed in Kemp's ridley turtles was near the minimum Ba:Ca ratio observed in loggerhead turtles (Figs. 3 & 4), which suggests differences in environmental availability or elemental uptake between the 2 species. The species otherwise had similar Mg:Ca and Sr:Ca ratios.

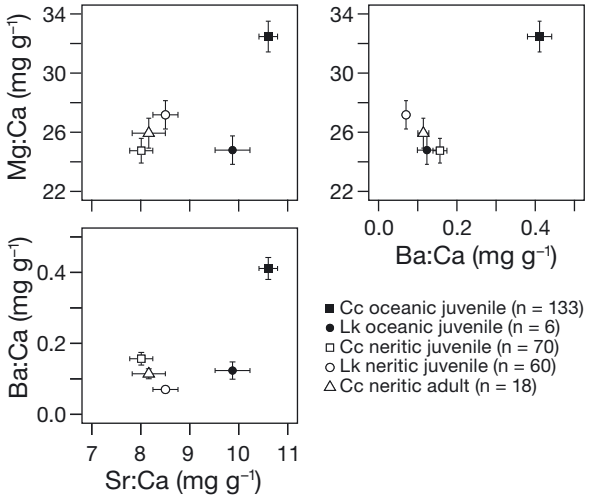

Fig. 4. Biplots of mean (±95% CI) life stage-specific Mg:Ca, Sr:Ca, and Ba:Ca ratios for loggerhead (Cc) and Kemp's ridley (Lk) sea turtles. Filled symbols are oceanic life stages; open symbols are neritic life stages. Adult data are means of entire ablation transects, whereas juvenile data are means of individual growth increments

3.3. Relationship between $\delta^{15}N$ values and trace element ratios

Given the apparent inverse patterns in $\delta^{15}N$ values and Mg:Ca, Sr:Ca, and Ba:Ca ratios, correlation analyses were used to quantify their relationships (Fig. 5, Table S4). For loggerhead turtles, $\delta^{15}N$ values exhibited a strong negative correlation with the Sr:Ca ratios and log(Ba:Ca) (r_{rm} = −0.74 and −0.70) and a moderate negative correlation with log(Mg:Ca) (r_{rm} = −0.48). For Kemp's ridley turtles, $\delta^{15}N$ values exhibited a moderate negative correlation with the Sr:Ca ratios (r_{rm} = −0.50) but no correlation with log(Mg:Ca) and log(Ba:Ca) (r_{rm} = −0.09 and −0.19).

4. DISCUSSION

We observed pronounced decreases in bone Sr:Ca and Ba:Ca ratios, and in some cases the Mg:Ca ratios, with increasing body size in loggerhead sea turtles and age in Kemp's ridley sea turtles. These changes coincided with increases in bone $\delta^{15}N$ values, an indicator of oceanic versus neritic resource use for these species, and occurred at sizes and ages typical of the oceanic-to-neritic shift. Bone $\delta^{15}N$ values and elemental ratios were distinct between life stages, plateauing at either high ($\delta^{15}N$ values) or low (trace element) values following the perceived ontogenetic shift. Ontogenetic changes in elemental ratios were

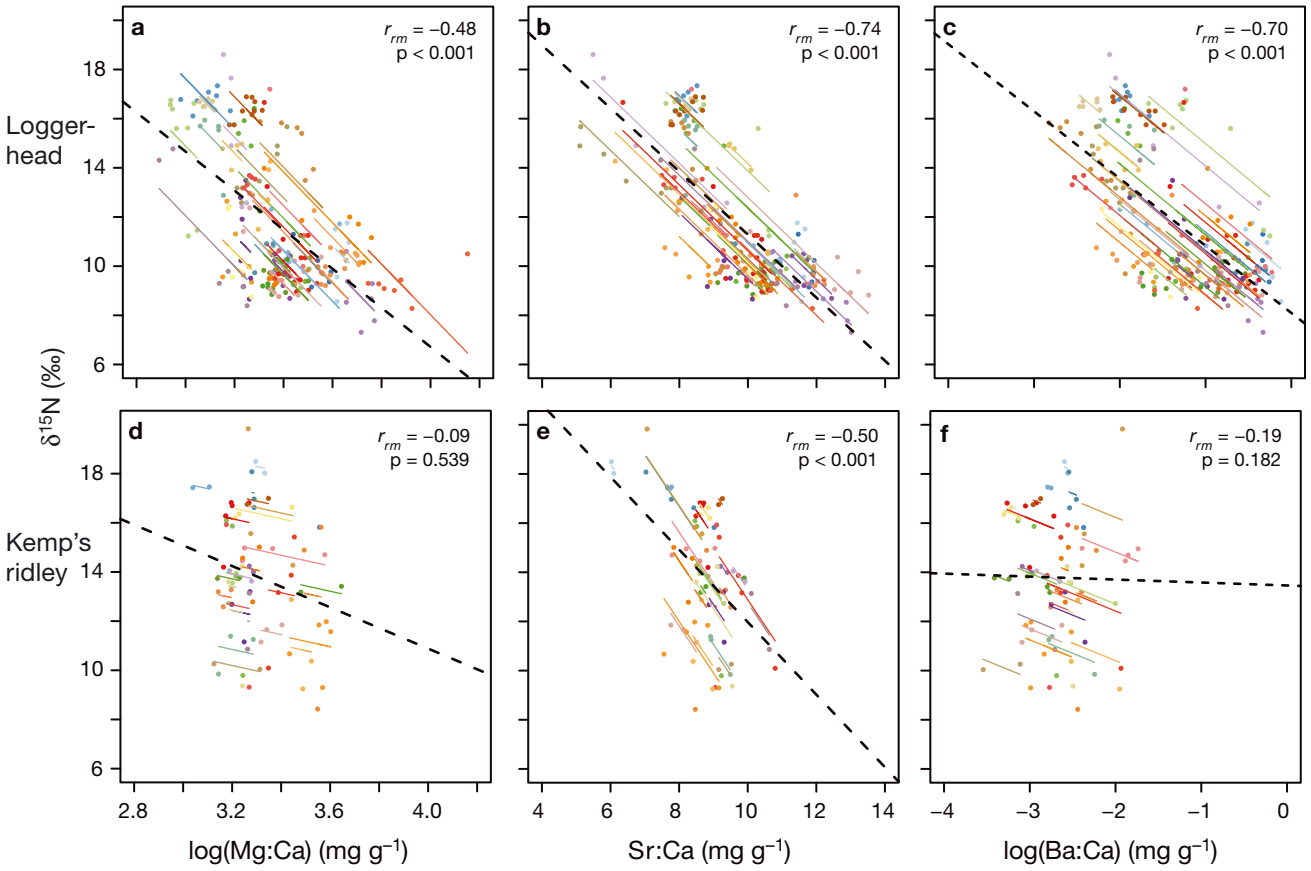

Fig. 5. Repeated measures correlation between $\delta^{15}N$ values and elemental ratios for (a–c) juvenile loggerhead (n = 35) and (d–f) juvenile Kemp's ridley (n = 28) sea turtles. Colored points are data for individual growth increments grouped by turtle. Colored lines are best linear fits for each turtle. The black dashed line is the overall model fit. Associated repeated measures correlation coefficients (r_{rm}, −1 to 1) and p-values are provided in each panel. Full statistical output is presented in Table S4 in the Supplement

greater in loggerhead turtles than Kemp's ridley turtles. Taken together, these results demonstrate the potential utility of Sr:Ca and Ba:Ca, and possibly Mg:Ca, ratios to reconstruct oceanic versus neritic resource use in these species, particularly for loggerhead turtles. Although our analyses uncovered novel relationships between biogeochemical and ontogenetic data in sea turtles, considerable variation in isotopic and elemental ratios remains unexplained in our analyses, highlighting the need to identify and investigate other factors influential to elemental incorporation in bone for these species.

The observed elemental patterns do not fully conform to expectations based on global chemical patterns in aquatic systems. Mg and Sr concentrations are generally homogeneous within the surface ocean (de Villiers 1999, Foster et al. 2010), and would thus be expected to be similarly homogeneous in surface-dwelling marine consumers, such as sea turtles, if elemental deposition were primarily a function of environmental availability. The declines in Sr:Ca ratios with increasing size/age observed herein were thus unexpected and suggest either that neritic-stage loggerhead turtles occupy habitats with significant freshwater inputs (e.g. estuaries) or that Sr incorporation in turtle bone is either fully or partially under physiological control (e.g. growth and diet effects). Sr is generally more abundant at higher salinities (Zimmerman 2005), although some freshwater end-members can have Sr concentrations approaching or similar to those in seawater (Kraus & Secor 2004). Thus, migrations from marine to estuarine habitats could manifest as decreases in tissue Sr:Ca ratios if an animal moved deep into estuarine waters (i.e. salinity <10 psu). Although such a pattern has been documented in Indian catfish *Plicofollis tenuispinis* that migrate from coastal to estuarine habitats (Kubota et al. 2015) and is evident in comparisons of otolith Sr:Ca ratios between estuarine and marine teleosts (Secor & Rooker 2000), this is unlikely to explain the

declines in Sr:Ca ratios observed in sea turtles. Neritic-stage sea turtles are not estuarine dependent, and are regularly documented throughout all parts of the US continental shelf (Mansfield et al. 2009, Shaver et al. 2013).

Ba, in contrast, exhibits greater spatiotemporal heterogeneity in the surface ocean, providing greater potential for discrimination of marine habitats, and is generally more abundant in freshwater versus saltwater (Coffey et al. 1997, Peek & Clementz 2012). Species migrating from marine to estuarine habitats may thus display the opposite pattern of Sr:Ca ratios, exhibiting increased Ba:Ca ratios with movements to nearshore habitats. Such patterns are evident in some fish species that migrate from coastal habitats to bays/estuaries (Hamer et al. 2006, Fowler et al. 2016) or open ocean to coastal habitats (Hamilton & Warner 2009, Baumann et al. 2015). These patterns were attributed to the input of Ba-rich freshwater or upwelled deep-water along continental margins. We thus expected the Ba:Ca ratios to possibly increase with movements from oceanic to neritic habitats, but instead observed decreases similar to the Sr:Ca ratios. To our knowledge, no other study has observed such patterns in the Ba:Ca ratios in species occupying the surface ocean. Sr:Ca and Ba:Ca ratios very often exhibit inverse relationships in fish otoliths. The fact that they are trending together in our study suggests that one or both are under strong physiological control, which may complicate their use as an environmental tracer of habitat use in sea turtles.

4.1. Trace element incorporation in bone tissue

Both environmental and physiological mechanisms can independently or synergistically control elemental deposition in the tissues of consumers, with temperature, growth, and diet having proven particularly influential. In fish, temperature can have positive, negative, and neutral effects on otolith Sr and Ba incorporation (e.g. Bath et al. 2000, Elsdon & Gillanders 2002, DiMaria et al. 2010). Similar studies are uncommon for calcium phosphate structures (e.g. bone), but both positive (fish bone; Balter & Lécuyer 2010) and negative (elasmobranch vertebrae; Smith et al. 2013) effects of temperature on Ba and Sr incorporation have been observed. Although similar studies are lacking for sea turtles, the observed patterns could be explained by positive temperature effects on elemental incorporation in turtle bone. Mansfield et al. (2014) found that thermal energy retention in *Sargassum* mats — habitats occupied by oceanic stage turtles — can raise local water temperatures by up to 6°C, well above those experienced in neritic stages. When combined with their float-and-wait foraging strategy (Witherington 2002, Witherington et al. 2012), this likely increases body temperatures and promotes food digestion and growth during the oceanic life stage. If we assume that temperature positively affects elemental incorporation in sea turtle bone, then we might expect increased Mg, Sr, and Ba uptake relative to Ca during the oceanic life stage similar to that observed in this study. Species-specific studies are needed to better understand the effect of temperature on elemental deposition rates in sea turtle bone.

The relationship between growth rate and elemental deposition in bone tissue is not well studied to date, and is confounded with temperature in ectotherms. In fish otoliths, higher growth rates have been associated with reduced Sr (Sadovy & Severin 1992, Walther et al. 2010, Sturrock et al. 2015) and possibly Ba (Miller 2011) uptake relative to Ca, but with increased Mg incorporation rates (Martin & Thorrold 2005, Sturrock et al. 2015, Limburg et al. 2018). Smith et al. (2013) compared vertebral elemental incorporation and somatic growth in elasmobranchs but found no significant relationships; thus, the temperature effects on Ba and Sr incorporation that they observed were independent of growth. Whether similar growth effects or non-effects occur in sea turtles is unknown. Nevertheless, it is unlikely that growth effects are the primary cause of the observed decreases in elemental ratios with size and age in these turtles, because growth rates are generally similar before and after the oceanic-to-neritic transition within each species, albeit with the exception of elevated growth during the year of transition in loggerhead turtles and the first year of life in Kemp's ridley turtles (Avens et al. 2017, Ramirez et al. 2017). However, growth effects may partially explain the differences in elemental ratios between species. Juvenile Kemp's ridley turtles grow twice as fast as juvenile loggerhead turtles of similar life stage (Avens et al. 2013, 2017). Therefore, if growth is negatively correlated with elemental incorporation rates in turtle bone as in fish otoliths, we would expect elemental ratios to be lower in Kemp's ridley turtles relative to loggerhead turtles, which we observed most clearly for Ba:Ca ratios at all life stages and Mg:Ca and Sr:Ca ratios during the oceanic life stage. Considering that neritic-stage loggerheads and Kemp's ridleys have overlapping spatial distributions, yet displayed different Ba:Ca ratios, there is the potential for growth effects or other species-specific factors to contribute to the observed differences between species.

Unlike fish, which deposit trace elements in otolith aragonite in proportion to what is present in the environment (Walther & Thorrold 2006), air-breathing animals deposit trace elements into bone hydroxyapatite in relation to what is present in their diet (Schroeder et al. 1972). Within both marine and terrestrial systems, physiological mechanisms discriminate against Sr and Ba during metabolic processing, resulting in decreasing Sr:Ca and Ba:Ca ratios with increasing trophic level (Burton et al. 1999, Peek & Clementz 2012). Therefore, an increase in foraging trophic level could also explain the decreases in elemental ratios observed herein. Although the simultaneous increases in $\delta^{15}N$ values would seem to support this idea, previous isotopic analyses have attributed this pattern primarily to differences in $\delta^{15}N$ values at the base of the food web rather than a shift in foraging trophic level (Ramirez et al. 2015). Loggerhead and Kemp's ridley sea turtles consume a primarily invertebrate diet that can be supplemented with fish discards from fisheries (Jones & Seminoff 2013), so diet effects could contribute to differences among individuals with divergent diets during neritic life stages. Nevertheless, trophic position estimates are lacking for these species, and more precise assessments of sea turtle diet and trophic ecology are needed to determine whether these patterns are related to changes in diet.

Clearly, further analyses are needed to better understand elemental deposition rates in sequentially deposited bone tissue. Cortical bone, the tissue sampled herein, has low turnover rates (~2% yr^{-1}; Parfitt 2002), so it is presumed that sea turtle humerus bone growth layers maintain stable chemical composition following bone formation until they are resorbed into the metabolically active core years later (Zug et al. 1986). However, the assimilation rate of diet constituents into consumer bone tissue is not well resolved. Two experimental studies in mammals provide some evidence that Sr deposition in bone occurs on the order of weeks to months. Bone Sr levels plateaued after 4 wk in continuously dosed rats (Dahl et al. 2001), whereas macaque *Macaca fascicularis* bone Sr levels only halved 10 wk following cessation of Sr treatment (Farlay et al. 2005). Although similar studies are lacking for reptiles, $\delta^{15}N$ values of yearling loggerhead scute tissue, a sequentially deposited tissue similar to bone, may take 2–4 mo to equilibrate with diet (Reich et al. 2008). We do not make any assumptions regarding elemental deposition rates in this study. However, applications of these methods for a more precise estimation of resource shifts will need to consider this and other influential factors when interpreting data.

4.2. Potential applications to life history reconstruction

In the future, trace element analyses conducted via LA-ICP-MS may provide a means of more precisely identifying the timing of ontogenetic shifts in sea turtles and possibly other marine megafauna. Recent bone stable isotope analyses ($\delta^{13}C$, $\delta^{15}N$) have improved stage duration estimation in sea turtles (Avens et al. 2013, Ramirez et al. 2015, Turner Tomaszewicz et al. 2017), but sample requirements necessitate integration of isotopic—and life history—information over an entire growth year. LA-ICP-MS, on the other hand, can provide a sub-annual chemical record that may further improve precision for life stage duration estimation if mechanisms underpinning elemental incorporation can be identified. For example, future studies could identify specific points within sea turtle bone growth layers where sharp chemical changes occur, to determine when within a growth year an individual transitioned between oceanic and neritic life stages. This would be possible because individual elemental profiles often exhibit distinct changes (Fig. 1, and see Fig. S2) that are masked in population-wide comparisons due to intraspecific variation in the timing of ontogenetic shifts. This could be valuable for understanding migration patterns between summer and winter foraging areas, or even identifying the frequency of reproduction for adults. Translating such information to calendar months or seasons will require a greater understanding of seasonal growth patterns and elemental incorporation rates, but could greatly expand our understanding of variation in resource use within and among life stages.

Additional studies are needed to confirm our results, investigate factors influencing elemental deposition in bone, and expand our understanding of chemical heterogeneity in marine habitats. Given the difficulty of studying highly migratory marine megafauna, controlled studies of captive marine animals or closely related terrestrial species will be key to unraveling the effects of environmental and physiological factors on elemental incorporation rates in bone tissue. Studies of natural populations will require novel integrations of new and existing technologies and methods in cross-discipline collaborations, such as in this study. Combining trace element analyses with geolocation tools and additional biogeochemical analyses (e.g. $\delta^{18}O$, Pb, compound-specific isotope analysis) could expand the utility and applicability of this method, as will further development of and integration with regional isoscapes (McMahon et al. 2013, Vander Zanden et al. 2015, Ceriani et al. 2017).

4.3. Conclusion

Trace element analysis and LA-ICP-MS are well-established methods for reconstruction of habitat use and movement in aquatic systems, but fewer studies have extended these methods to non-fish species. Here we outline the first application of trace element analysis conducted via LA-ICP-MS to the study of ontogenetic resource use in marine reptiles. We demonstrate the potential value of multiple elemental ratios, but particularly Ba:Ca and Sr:Ca ratios, to the reconstruction of oceanic-to-neritic ontogenetic shifts in loggerhead and Kemp's ridley sea turtles within the North Atlantic Ocean. Additional research is needed to quantify the effect of environmental and physiological factors on elemental incorporation rates in these species. Expanded study of elemental ratios in Kemp's ridley bones is also needed, particularly during the oceanic life stage, to clarify relationships in this species. Although we conducted this work on sea turtles, we believe these methods may be applicable to the study of other highly migratory marine animals, such as marine mammals, that migrate between coastal and open ocean habitats.

Acknowledgements. We thank the participants of the National Sea Turtle Stranding and Salvage Network for their dedicated work. We also thank J. McKay for processing all stable isotope samples, A. Ungerer and B. Pitcher for assistance with LA-ICP-MS, K. Bankston for assistance with micromilling, and A. Goodman Hall for assistance with bone section imaging. This publication was made possible by the NSF Graduate Research Fellowship Program and the National Oceanic and Atmospheric Administration, Office of Education Educational Partnership Program. Its contents are solely the responsibility of the authors and do not necessarily represent the official views of the U.S. Department of Commerce, National Oceanic and Atmospheric Administration. Research was conducted under USFWS permit number TE-676379-5 issued to the NMFS Southeast Fisheries Science Center. Thank you to S. Arbuckle, T. Garcia, S.A. Heppell, P. Kappes, and C. Murphy, H. Baumann, and 2 anonymous reviewers for their help in improving this manuscript.

LITERATURE CITED

Avens L, Snover ML (2013) Age and age estimation in sea turtles. In: Wyneken J, Lohmann KJ, Musick JA (eds) The biology of sea turtles. CRC Press, Boca Raton, FL, p 97–134

Avens L, Goshe LR, Pajuelo M, Bjorndal KA and others (2013) Complementary skeletochronology and stable isotope analyses offer new insight into juvenile loggerhead sea turtle oceanic stage duration and growth dynamics. Mar Ecol Prog Ser 491:235–251

Avens L, Goshe LR, Coggins L, Snover ML, Pajuelo M, Bjorndal KA, Bolten AB (2015) Age and size at maturation- and adult-stage duration for loggerhead sea turtles in the western North Atlantic. Mar Biol 162:1749–1767

Avens L, Goshe LR, Coggins L, Shaver DJ, Higgins B, Landry AM, Bailey R (2017) Variability in age and size at maturation, reproductive longevity, and long-term growth dynamics for Kemp's ridley sea turtles in the Gulf of Mexico. PLOS ONE 12:e0173999

Bakdash JZ, Marusich LR (2017) Repeated measures correlation. Front Psychol 8:456

Balter V, Lécuyer C (2010) Determination of Sr and Ba partition coefficients between apatite from fish (*Sparus aurata*) and seawater: the influence of temperature. Geochim Cosmochim Acta 74:3449–3458

Bath GE, Thorrold SR, Jones CM, Campana SE, McLaren JW, Lam JWH (2000) Strontium and barium uptake in aragonitic otoliths of marine fish. Geochim Cosmochim Acta 64:1705–1714

Baumann H, Wells RJD, Rooker JR, Zhang S and others (2015) Combining otolith microstructure and trace elemental analyses to infer the arrival of juvenile Pacific bluefin tuna in the California current ecosystem. ICES J Mar Sci 72:2128–2138

Bjorndal KA, Bolten AB, Martins HR (2000) Somatic growth model of juvenile loggerhead sea turtles *Caretta caretta*: duration of pelagic stage. Mar Ecol Prog Ser 202:265–272

Block BA, Jonsen ID, Jorgensen SJ, Winship AJ and others (2011) Tracking apex marine predator movements in a dynamic ocean. Nature 475:86–90

Bolten AB (2003) Variation in sea turtle life history patterns: neritic vs. oceanic developmental stages. In: Lutz PL, Musick JA, Wyneken J (eds) The biology of sea turtles. CRC Press, Boca Raton, FL, p 243–273

Born EW, Outridge P, Riget FF, Hobson KA, Dietz R, Øien N, Haug T (2003) Population substructure of North Atlantic minke whales (*Balaenoptera acutorostrata*) inferred from regional variation of elemental and stable isotopic signatures in tissues. J Mar Syst 43:1–17

Botta S, Albuquerque C, Hohn AA, da Silva VMF and others (2015) Ba/Ca ratios in teeth reveal habitat use patterns of dolphins. Mar Ecol Prog Ser 521:249–263

Brennan SR, Zimmerman CE, Fernandez DP, Cerling TE, McPhee MV, Wooller MJ (2015) Strontium isotopes delineate fine-scale natal origins and migration histories of Pacific salmon. Sci Adv 1:e1400124

Burton JH, Price TD, Middleton WD (1999) Correlation of bone Ba/Ca and Sr/Ca due to biological purification of calcium. J Archaeol Sci 26:609–616

Campana SE (1999) Chemistry and composition of fish otoliths: pathways, mechanisms and applications. Mar Ecol Prog Ser 188:263–297

Campana SE, Thorrold SR (2001) Otoliths, increments, and elements: keys to a comprehensive understanding of fish populations? Can J Fish Aquat Sci 58:30–38

Campana SE, Fowler AJ, Jones CM (1994) Otolith elemental fingerprinting for stock identification of Atlantic cod (*Gadus morhua*) using laser ablation ICPMS. Can J Fish Aquat Sci 51:1942–1950

Carr A (1952) Handbook of turtles: the turtles of the United States, Canada, and Baja California. Cornell University Press, Ithaca, NY

Ceriani SA, Weishampel JF, Ehrhart LM, Mansfield KL, Wunder MB (2017) Foraging and recruitment hotspot dynamics for the largest Atlantic loggerhead turtle rookery. Sci Rep 7:16894

Chang MY, Geffen AJ (2013) Taxonomic and geographic

influences on fish otolith microchemistry. Fish Fish 14: 458–492
Coffey M, Dehairs F, Collette O, Luther G, Church T, Jickells T (1997) The behaviour of dissolved barium in estuaries. Estuar Coast Shelf Sci 45:113–121
Dahl SG, Allain P, Marie PJ, Mauras Y and others (2001) Incorporation and distribution of strontium in bone. Bone 28:446–453
de Villiers S (1999) Seawater strontium and Sr/Ca variability in the Atlantic and Pacific oceans. Earth Planet Sci Lett 171:623–634
DiMaria RA, Miller JA, Hurst TP (2010) Temperature and growth effects on otolith elemental chemistry of larval Pacific cod, *Gadus macrocephalus.* Environ Biol Fishes 89:453–462
Dodge KL, Galuardi B, Miller TJ, Lutcavage ME (2014) Leatherback turtle movements, dive behavior, and habitat characteristics in ecoregions of the Northwest Atlantic Ocean. PLOS ONE 9:e91726
Dorado S, Rooker JR, Wissel B, Quigg A (2012) Isotope baseline shifts in pelagic food webs of the Gulf of Mexico. Mar Ecol Prog Ser 464:37–49
Edmonds JS, Caputi N, Morita M (1991) Stock discrimination by trace-element analysis of otoliths of orange roughy (*Hoplostethus atlanticus*), a deep-water marine teleost. Aust J Mar Freshw Res 42:383–389
Elsdon TS, Gillanders BM (2002) Interactive effects of temperature and salinity on otolith chemistry: challenges for determining environmental histories of fish. Can J Fish Aquat Sci 59:1796–1808
Elsdon TS, Gillanders BM (2003) Reconstructing migratory patterns of fish based on environmental influences on otolith chemistry. Rev Fish Biol Fish 13:217–235
Elsdon TS, Wells BK, Campana SE, Gillanders BM and others (2008) Otolith chemistry to describe movements and life-history parameters of fishes. Oceanogr Mar Biol Annu Rev 46:297–330
Farlay D, Boivin G, Panczer G, Lalande A, Meunier PJ (2005) Long-term strontium ranelate administration in monkeys preserves characteristics of bone mineral crystals and degree of mineralization of bone. J Bone Miner Res 20:1569–1578
Fontaine MC, Tolley KA, Siebert U, Gobert S, Lepoint G, Bouquegneau JM, Das K (2007) Long-term feeding ecology and habitat use in harbour porpoises *Phocoena phocoena* from Scandinavian waters inferred from trace elements and stable isotopes. BMC Ecol 7:1
Foster GL, Pogge von Strandmann PAE, Rae JWB (2010) Boron and magnesium isotopic composition of seawater. Geochem Geophys Geosystems 11:Q08015
Fowler AM, Smith SM, Booth DJ, Stewart J (2016) Partial migration of grey mullet (*Mugil cephalus*) on Australia's east coast revealed by otolith chemistry. Mar Environ Res 119:238–244
Francis R (1990) Back-calculation of fish length: a critical review. J Fish Biol 36:883–902
Goodman Hall AG, Avens L, Braun McNeill J, Wallace B, Goshe LR (2015) Inferring long-term foraging trends of individual juvenile loggerhead sea turtles using stable isotopes. Mar Ecol Prog Ser 537:265–276
Hamer PA, Jenkins GP, Coutin P (2006) Barium variation in *Pagrus auratus* (Sparidae) otoliths: a potential indicator of migration between an embayment and ocean waters in south-eastern Australia. Estuar Coast Shelf Sci 68: 686–702
Hamilton SL, Warner RR (2009) Otolith barium profiles verify the timing of settlement in a coral reef fish. Mar Ecol Prog Ser 385:237–244
Hobson KA (2007) Isotopic tracking of migrant wildlife. In: Michener RH, Lajtha K (eds) Stable isotopes in ecology and environmental science. Blackwell Publishing, Malden, MA, p 155–175
Hothorn T, Bretz F, Westfall P (2008) Simultaneous inference in general parametric models. Biom J 50:346–363
Jochum KP, Weis U, Stoll B, Kuzmin D and others (2011) Determination of reference values for NIST SRM 610-617 glasses following ISO guidelines. Geostand Geoanal Res 35:397–429
Jones TT, Seminoff JA (2013) Feeding biology: advances from field-based observations, physiological studies, and molecular techniques. In: Wyneken J, Lohmann KJ, Musick JA (eds) The biology of sea turtles. CRC Press, Boca Raton, FL, p 211–247
Kalish JM (1991) Determinants of otolith chemistry: seasonal variation in the composition of blood plasma, endolymph and otoliths of bearded rock cod *Pseudophycis barbatus.* Mar Ecol Prog Ser 74:137–159
Kent AJR, Ungerer CA (2006) Analysis of light lithophile elements (Li, Be, B) by laser ablation ICP-MS: comparison between magnetic sector and quadrupole ICP-MS. Am Mineral 91:1401–1411
Koch PL, Fogel ML, Tuross N (1994) Tracing the diets of fossil animals using stable isotopes. In: Lajtha K, Michener RH (eds) Stable isotopes in ecology and environmental science. Blackwell, Boston, MA, p 63–92
Kraus RT, Secor DH (2004) Incorporation of strontium into otoliths of an estuarine fish. J Exp Mar Biol Ecol 302: 85–106
Kubota K, Yokoyama Y, Kawakubo Y, Seki A and others (2015) Migration history of an ariid Indian catfish reconstructed by otolith Sr/Ca and $\delta^{18}O$ micro-analysis. Geochem J 49:469–480
Kunito T, Watanabe I, Yasunaga G, Fujise Y, Tanabe S (2002) Using trace elements in skin to discriminate the populations of minke whales in southern hemisphere. Mar Environ Res 53:175–197
Limburg KE, Wuenschel MJ, Hüssy K, Heimbrand Y, Samson M (2018) Making the otolith magnesium chemical calendar-clock tick: plausible mechanism and empirical evidence. Rev Fish Sci Aquacult 26:479–493
López-Castro MC, Bjorndal KA, Kamenov GD, Zenil-Ferguson R, Bolten AB (2013) Sea turtle population structure and connections between oceanic and neritic foraging areas in the Atlantic revealed through trace elements. Mar Ecol Prog Ser 490:233–246
López-Castro MC, Bjorndal KA, Kamenov GD, Bolten AB (2014) Identifying oceanic foraging grounds of sea turtles in the Atlantic using lead isotopes. Mar Biol 161: 2269–2278
Mansfield KL, Saba VS, Keinath JA, Musick JA (2009) Satellite tracking reveals a dichotomy in migration strategies among juvenile loggerhead turtles in the Northwest Atlantic. Mar Biol 156:2555–2570
Mansfield KL, Wyneken J, Porter WP, Luo J (2014) First satellite tracks of neonate sea turtles redefine the 'lost years' oceanic niche. Proc R Soc B 281:20133039
Martin GB, Thorrold SR (2005) Temperature and salinity effects on magnesium, manganese, and barium incorporation in otoliths of larval and early juvenile spot *Leiostomus xanthurus.* Mar Ecol Prog Ser 293:223–232

McClellan CM, Read AJ (2007) Complexity and variation in loggerhead sea turtle life history. Biol Lett 3:592–594
McKinney RA, Oczkowski AJ, Prezioso J, Hyde KJW (2010) Spatial variability of nitrogen isotope ratios of particulate material from Northwest Atlantic continental shelf waters. Estuar Coast Shelf Sci 89:287–293
McMahon KW, Hamady LL, Thorrold SR (2013) A review of ecogeochemistry approaches to estimating movements of marine animals. Limnol Oceanogr 58:697–714
McMillan MN, Izzo C, Wade B, Gillanders BM (2017) Elements and elasmobranchs: hypotheses, assumptions and limitations of elemental analysis. J Fish Biol 90:559–594
Michener RH, Kaufman L (2007) Stable isotope ratios as tracers in marine food webs: an update. In: Michener RH, Lajtha K (eds) Stable isotopes in ecology and environmental science. Blackwell Publishing, Malden, MA, p 238–282
Miller JA (2007) Scales of variation in otolith elemental chemistry of juvenile staghorn sculpin (*Leptocottus armatus*) in three Pacific Northwest estuaries. Mar Biol 151:483–494
Miller JA (2011) Effects of water temperature and barium concentration on otolith composition along a salinity gradient: implications for migratory reconstructions. J Exp Mar Biol Ecol 405:42–52
Montoya JP, Carpenter EJ, Capone DG (2002) Nitrogen fixation and nitrogen isotope abundances in zooplankton of the oligotrophic North Atlantic. Limnol Oceanogr 47: 1617–1628
Moran JJ, Newburn MK, Alexander ML, Sams RL, Kelly JF, Kreuzer HW (2011) Laser ablation isotope ratio mass spectrometry for enhanced sensitivity and spatial resolution in stable isotope analysis. Rapid Commun Mass Spectrom 25:1282–1290
Outridge PM, Stewart RE (1999) Stock discrimination of Atlantic walrus (*Odobenus rosmarus rosmarus*) in the eastern Canadian Arctic using lead isotope and element signatures in teeth. Can J Fish Aquat Sci 56:105–112
Parfitt AM (2002) Misconceptions (2): Turnover is always higher in cancellous than in cortical bone. Bone 30: 807–809
Pearson R, van de Merwe J, Limpus C, Connolly R (2017) Realignment of sea turtle isotope studies needed to match conservation priorities. Mar Ecol Prog Ser 583: 259–271
Peek S, Clementz MT (2012) Sr/Ca and Ba/Ca variations in environmental and biological sources: a survey of marine and terrestrial systems. Geochim Cosmochim Acta 95: 36–52
Peterson BJ, Fry B (1987) Stable isotopes in ecosystem studies. Annu Rev Ecol Syst 18:293–320
Pinheiro J, Bates D, DebRoy S, Sarkar D, R Core Team (2018) nlme: linear and nonlinear mixed effects models. R package version 3.1-137. https://CRAN.R-project.org/package=nlme
Post DM, Layman CA, Arrington DA, Takimoto G, Quattrochi J, Montaña CG (2007) Getting to the fat of the matter: models, methods and assumptions for dealing with lipids in stable isotope analyses. Oecologia 152:179–189
R Core Team (2018) R: a language and environment for statistical computing. R Foundation for Statistical Computing, Vienna
Ramirez MD, Avens L, Seminoff JA, Goshe LR, Heppell SS (2015) Patterns of loggerhead turtle ontogenetic shifts revealed through isotopic analysis of annual skeletal growth increments. Ecosphere 6:244
Ramirez MD, Avens L, Seminoff JA, Goshe LR, Heppell SS (2017) Growth dynamics of juvenile loggerhead sea turtles undergoing an ontogenetic habitat shift. Oecologia 183:1087–1099
Reich KJ, Bjorndal KA, Bolten AB (2007) The 'lost years' of green turtles: using stable isotopes to study cryptic lifestages. Biol Lett 3:712–714
Reich KJ, Bjorndal KA, Martínez del Rio C (2008) Effects of growth and tissue type on the kinetics of ^{13}C and ^{15}N incorporation in a rapidly growing ectotherm. Oecologia 155:651–663
Romero MB, Polizzi P, Chiodi L, Robles A, Das K, Gerpe M (2017) Metals as chemical tracers to discriminate ecological populations of threatened Franciscana dolphins (*Pontoporia blainvillei*) from Argentina. Environ Sci Pollut Res Int 24:3940–3950
Rubenstein DR, Hobson KA (2004) From birds to butterflies: animal movement patterns and stable isotopes. Trends Ecol Evol 19:256–263
Sadovy Y, Severin KP (1992) Trace elements in biogenic aragonite: correlation of body growth rate and strontium levels in the otoliths of the white grunt, *Haemulon plumieri* (Pisces: Haemulidae). Bull Mar Sci 50:237–257
Schroeder HA, Tipton IH, Nason AP (1972) Trace metals in man: strontium and barium. J Chronic Dis 25:491–517
Secor DH, Rooker JR (2000) Is otolith strontium a useful scalar of life cycles in estuarine fishes? Fish Res 46: 359–371
Shaver DJ, Hart KM, Fujisaki I, Rubio C and others (2013) Foraging area fidelity for Kemp's ridleys in the Gulf of Mexico. Ecol Evol 3:2002–2012
Smith WD, Miller JA, Heppell SS (2013) Elemental markers in elasmobranchs: effects of environmental history and growth on vertebral chemistry. PLOS ONE 8:e62423
Snover ML (2002) Growth and ontogeny of sea turtles using skeletochronology: methods, validation and application to conservation. PhD dissertation, Duke University, Durham, NC
Snover ML, Hohn AA (2004) Validation and interpretation of annual skeletal marks in loggerhead (*Caretta caretta*) and Kemp's ridley (*Lepidochelys kempii*) sea turtles. Fish Bull 102:682–692
Snover ML, Avens L, Hohn AA (2007a) Back-calculating length from skeletal growth marks in loggerhead sea turtles *Caretta caretta.* Endang Species Res 3:95–104
Snover ML, Hohn AA, Crowder LB, Heppell SS (2007b) Age and growth in Kemp's ridley sea turtles: evidence from mark-recapture and skeletochronology. In: Plotkin PT (ed) Biology and conservation of ridley sea turtles. Johns Hopkins University Press, Baltimore, MD, p 89–106
Snover ML, Hohn AA, Crowder LB, Macko SA (2010) Combining stable isotopes and skeletal growth marks to detect habitat shifts in juvenile loggerhead sea turtles *Caretta caretta.* Endang Species Res 13:25–31
Sturrock AM, Trueman CN, Darnaude AM, Hunter E (2012) Can otolith elemental chemistry retrospectively track migrations in fully marine fishes? J Fish Biol 81:766–795
Sturrock AM, Hunter E, Milton JA, EIMF, Johnson RC, Waring CP, Trueman CN (2015) Quantifying physiological influences on otolith microchemistry. Methods Ecol Evol 6:806–816
Thorrold SR, Latkoczy C, Swart PK, Jones CM (2001) Natal homing in a marine fish metapopulation. Science 291: 297–299

Turner Tomaszewicz CN, Seminoff JA, Ramirez MD, Kurle CM (2015) Effects of demineralization on the stable isotope analysis of bone samples. Rapid Commun Mass Spectrom 29:1879–1888

Turner Tomaszewicz CN, Seminoff JA, Peckham SH, Avens L, Kurle CM (2017) Intrapopulation variability in the timing of ontogenetic habitat shifts in sea turtles revealed using $\delta^{15}N$ values from bone growth rings. J Anim Ecol 86:694–704

Turtle Expert Working Group (2000) Assessment update for the Kemp's ridley and loggerhead sea turtle populations in the Western North Atlantic. Tech Mem NMFS-SEFSC-444. U.S. Department of Commerce, NOAA,

Vander Zanden HB, Tucker AD, Hart KM, Lamont MM and others (2015) Determining origin in a migratory marine vertebrate: a novel method to integrate stable isotopes and satellite tracking. Ecol Appl 25:320–335

Walther BD, Thorrold SR (2006) Water, not food, contributes the majority of strontium and barium deposited in the otoliths of a marine fish. Mar Ecol Prog Ser 311:125–130

Walther BD, Kingsford MJ, O'Callaghan MD, McCulloch MT (2010) Interactive effects of ontogeny, food ration and temperature on elemental incorporation in otoliths of a coral reef fish. Environ Biol Fishes 89:441–451

Wells RJD, Rooker JR (2009) Feeding ecology of pelagic fish larvae and juveniles in slope waters of the Gulf of Mexico. J Fish Biol 75:1719–1732

Wilmers CC, Nickel B, Bryce CM, Smith JA, Wheat RE, Yovovich V (2015) The golden age of bio-logging: how animal-borne sensors are advancing the frontiers of ecology. Ecology 96:1741–1753

Witherington B (2002) Ecology of neonate loggerhead turtles inhabiting lines of downwelling near a Gulf Stream front. Mar Biol 140:843–853

Witherington B, Hirama S, Hardy R (2012) Young sea turtles of the pelagic *Sargassum*-dominated drift community: habitat use, population density, and threats. Mar Ecol Prog Ser 463:1–22

Witzell WN (2002) Immature Atlantic loggerhead turtles (*Caretta caretta*): suggested changes to the life history model. Herpetol Rev 33:266–269

Wood SN (2006) Generalized additive models: an introduction with R. Chapman and Hall/CRC Press, Boca Raton, FL

Zimmerman CE (2005) Relationship of otolith strontium-to-calcium ratios and salinity: experimental validation for juvenile salmonids. Can J Fish Aquat Sci 62:88–97

Zug GR, Wynn AH, Ruckdeschel C (1986) Age determination of loggerhead sea turtles, *Caretta caretta*, by incremental growth marks in the skeleton. Smithson Contrib Zool 427:1–44

Zug GR, Kalb HJ, Luzar SJ (1997) Age and growth in wild Kemp's ridley sea turtles *Lepidochelys kempii* from skeletochronological data. Biol Conserv 80:261–268

Editorial responsibility: Keith Hobson, London, Ontario, Canada

Submitted: March 7, 2018; Accepted: October 22, 2018
Proofs received from author(s): December 6, 2018